

RESEARCH PAPER

## Influence of the Size of Micronized Active Pharmaceutical Ingredient on the Aerodynamic Particle Size and Stability of a Metered Dose Inhaler

Julianne Berry, Ph.D.,\* Lukeysha C. Kline, B.A., Jill K. Sherwood, Ph.D.,  
Saeed Chaudhry, M.S., Linda Obenauer-Kutner, M.S.,  
John L. Hart, Ph.D., and Joel Sequeira, Ph.D.

Schering-Plough Research Institute, Kenilworth, New Jersey, USA

### ABSTRACT

Pharmaceutical inhalers are often used to treat pulmonary diseases. Only active pharmaceutical ingredient (API) particles from these inhalers that are less than approximately 5  $\mu\text{m}$  are likely to reach the lung and be efficacious. This study was designed to investigate the impact of micronized API particle size on the aerodynamic particle size distribution (PSD) profile and the particle size stability of a suspension metered dose inhaler (MDI) containing propellant HFA-227 (1,1,1,2,3,3,3 heptafluoropropane) and a corticosteroid. The median API particle size ranged from 1.1  $\mu\text{m}$  to 1.8  $\mu\text{m}$  (97% to 70% of particles <3  $\mu\text{m}$ , respectively). This study showed that increasing the particle size of the API used to manufacture a suspension MDI product increased the aerodynamic PSD of the MDI product. Furthermore, upon storage of the MDI product under temperature cycling conditions, samples containing larger-size API particles were less stable with respect to their aerodynamic PSD than those with smaller-size API particles. It was found that size-dependent particle growth and/or aggregation of the suspended API may be occurring as a result of temperature cycling. In conclusion, this study has shown that the particle size of the raw API impacts the properties and stability of the emitted aerosol spray. Based on the findings from this study, it is recommended that the API particle size be carefully controlled in order to meet specifications set for the finished MDI product.

*Key Words:* Cascade impaction; Particle size distribution (PSD); Metered dose inhalers (MDI); Sympatec laser diffraction; Micronization; Aerosol; Temperature cycling.

\*Correspondence: Julianne Berry, Ph.D., Schering-Plough Research Institute, 2000 Galloping Hill Rd., Kenilworth, NJ 07033, USA; E-mail: julianne.berry@spcorp.com.

## INTRODUCTION

A metered dose inhaler (MDI) used in the treatment of pulmonary diseases<sup>[1–3]</sup> is often comprised of micronized active pharmaceutical ingredient (API) suspended in a propellant-based liquid medium. The MDI device consisting of a metered valve, can, and actuator is designed to provide a fine droplet spray for inhalation therapy. The efficacy of the emitted dose, which is determined by the amount of API that reaches the lungs, is related to the aerodynamic particle size distribution (PSD) of the inhaled spray droplets.<sup>[4–7]</sup>

In an environment where sufficient evaporation of the volatile liquid component of the spray droplet can occur, the aerodynamic particle size profile of the inhaled spray of a suspension MDI is likely to be dependent on the size of the API.<sup>[8]</sup> For a heptafluoropropane (HFA)-based oral MDI that was tested by cascade impaction using an entry port that allows for high evaporation of the spray droplets, the aerodynamic PSD of products containing fine and coarse API could be distinguished.<sup>[9,10]</sup>

Because the spray droplets may be sensitive to the size of the API, then it follows that changes in API particle size over time could impact the particle size stability of the formulation and, therefore, the amount of API that reaches the lungs. A solid suspended in a liquid medium has the propensity to undergo particle growth or aggregation, especially under conditions of supersaturation, agitation, and changes in environmental conditions.<sup>[11–18]</sup> If the API particles suspended in the MDI increase in size (e.g., by particle growth or aggregation) during storage, then these changes could be manifested in an increase in the aerodynamic PSD of the emitted dose.

In view of the fact that the API particle size could be a critical parameter in the performance and stability

of the MDI, it was the goal of this study to evaluate its impact on the aerodynamic PSD and stability using a model HFA formulation. An HFA-based system was selected because it is employed in most new MDIs, making this information beneficial for the development of new MDI products. The HFA MDI systems have unique physical and chemical properties that have resulted in differences in the spray dynamics from that of the chlorofluorocarbon (CFC) predecessors.<sup>[19–23]</sup>

The API particle size used in this study was achieved through jet-mill micronization of the recrystallized material. Jet-mill micronization is a particle size reduction method typically used to produce a particle size range of approximately 1 to 5  $\mu\text{m}$  required for most inhalation products.<sup>[24–26]</sup> The micronizer serves to make particles smaller as well as smoother and rounder through the energy from a high-velocity air stream, which causes high-energy particle collisions.<sup>[27]</sup> The resultant particle size is dependent on micronizer operating conditions such as powder feed rate and applied pressure.<sup>[24–26]</sup>

## MATERIALS AND METHODS

### Description and Characterization of API

Recrystallized API (corticosteroid) was micronized using the standard jet-mill micronizer.<sup>[25,26]</sup> An inverse relationship was observed between the operating feed rate and the resulting particle size of the micronized material. API lots used in this investigation ranged in median particle size from 1.1  $\mu\text{m}$  to 1.8  $\mu\text{m}$ .

The PSD profile of the API (Table 1) was measured directly in the laser diffraction beam as an aerosolized dry powder using the RODOS dry powder accessory (Sympatec HELOS Compact, model KA

**Table 1.** API particle size by Sympatec laser diffraction.<sup>a</sup>

API lot number	Median ( $\mu\text{m}$ )	Cumulative percent under size (%)		
		0.52 $\mu\text{m}$	1.20 $\mu\text{m}$	3.00 $\mu\text{m}$
1	1.14	16.7	53.2	97.2
2	1.19	18.1	50.7	92.7
3	1.25	17.8	48.2	88.1
4	1.38	13.9	44.4	83.3
5	1.53	14.9	40.3	77.4
6	1.77	13.2	35.9	69.9

<sup>a</sup>Sympatec Laser HELOS with RODOS dry powder accessory;  $n=2$ .

with a R2 helium–neon laser GmbH, Windox Software 3.0, Clausthal-Zellerfeld, Germany). Duplicate PSD measurements were obtained.

Using differential scanning calorimetry (DSC) thermograms (TI Model 2920, heating rate 10°C/min), the API was shown to be crystalline (limit of detection of amorphous content was about 1%).

Scanning electron microscopy (SEM; JEOL, Model JSM-5600LV with 3-kV beam) was used for the microscopic evaluation of the API.

### General Description of MDI Products

Each product batch contained micronized API, a surfactant (long-chain fatty acid), alcohol (ethanol), and propellant HFA-227. The alcohol level in the MDI was less than 5% w/w. The combined API and surfactant levels in the MDI were less than 0.2% w/w. About 10 g of the suspension was filled into a commercially available aerosol can that was crimped with a commercially available 63-μL valve.

The MDI was manufactured according to a standard method used for aerosol products. Immediately following batch manufacture, all samples were stored in the valve-down position for a period of about 2 weeks at ambient room conditions prior to testing at the initial time point. Previously, it had been shown that the swelling of the valve elastomers reaches equilibrium in this time period (unpublished data).

MDI product was initially manufactured for the purpose of determining the product particle size profile

as a function of the API lot (i.e., batches A through F in Table 2). These product batches contained API lots 1 to 6, respectively, which are described in Table 1.

Subsequently, two separate MDI product batches were manufactured for the purpose of determining the product particle size stability (i.e., batches G and H in Table 3). These product batches were manufactured by a modified manufacturing process, which tended to produce a finer MDI PSD than that used with batches A through F. Batch H contained API lot 1, which had a median particle size of about 1.1 μm (Table 1). Batch G contained a new API lot, which had a median particle size of about 1.3 μm.

### Temperature Cycling Stability of MDI Product

MDI product batches G and H (Table 3) were placed into a temperature cycling chamber (Model 3941, Forma Scientific, Inc., Marietta, OH) in the valve-down position and cycled from –10°C to 40°C, four times a day for 2 weeks at ambient humidity. Earlier studies of this model formulation showed that particle growth was promoted upon temperature cycling, whereas storage at ambient temperature and humidity over a period of at least 1 month did not change the PSD of this formulation (unpublished data). Visual inspection of the suspension at the temperature cycling storage condition revealed the tendency of the API to settle to the bottom of the suspension medium at 40°C and cream to the top of the suspension medium

**Table 2.** Initial MDI aerodynamic particle size results by Andersen Cascade Impaction.<sup>a,b</sup>

Batch label	Dose recovered in cascade impactor (%)	Distribution of dose in cascade impactor (%)	Fine particles, ≤ 4.7 μm (%)	MMAD <sup>c</sup> (μm) (GSD <sup>c</sup> )
A (API lot 1)	99±2	Stages: 90±1 Entry port: 6±1	79±2	2.58±0.05 (1.84±0.02)
B (API lot 2)	96±3	Stages: 89±2 Entry port: 6±2	76±4	2.63±0.06 (1.90±0.01)
C (API lot 3)	98±1	Stages: 89±2 Entry port: 6±2	68±1	2.83±0.05 (2.01±0.05)
D (API lot 4)	92±2	Stages: 85±1 Entry port: 9±1	58±1	3.09±0.10 (2.25±0.03)
E (API lot 5)	95±2	Stages: 83±2 Entry port: 10±1	50±3	3.54±0.16 (2.30±0.06)
F (API lot 6)	94±2	Stages: 78±1 Entry port: 13±1	38±2	4.38±0.20 (2.61±0.01)

<sup>a</sup>Described in the experimental section, *n*=3.

<sup>b</sup>Results presented as mean±standard deviation.

<sup>c</sup>Estimated based on USP method.

**Table 3.** MDI aerodynamic particle size results by Andersen Cascade Impaction—effect of temperature cycling.<sup>a,b</sup>

Batch label	Condition	Dose recovered in cascade impactor (%)	Distribution of dose in cascade impactor (%)	Fine particles, $\leq 4.7 \mu\text{m}$ (%)	MMAD <sup>c</sup> ( $\mu\text{m}$ ) (GSD <sup>c</sup> )
G (Coarse API)	Initial	94 $\pm$ 3	Stages: 86 $\pm$ 0 Entry port: 9 $\pm$ 0	62 $\pm$ 1	3.17 $\pm$ 0.00 (2.14 $\pm$ 0.01)
	2 wk/TC	96 $\pm$ 1	Stages: 72 $\pm$ 7 Entry port: 20 $\pm$ 5	30 $\pm$ 4	4.99 $\pm$ 0.15 (2.97 $\pm$ 0.12)
H (Fine API)	Initial	93 $\pm$ 2	Stages: 90 $\pm$ 0 Entry port: 7 $\pm$ 0	84 $\pm$ 0	2.30 $\pm$ 0.01 (1.84 $\pm$ 0.00)
	2 wk/TC	101 $\pm$ 5	Stages: 87 $\pm$ 2 Entry port: 9 $\pm$ 3	69 $\pm$ 1	2.73 $\pm$ 0.16 (2.00 $\pm$ 0.01)

<sup>a</sup>Described in the experimental section,  $n=3$ .<sup>b</sup>Results presented as mean $\pm$ standard deviation.<sup>c</sup>Estimated based on USP method.

at  $-10^{\circ}\text{C}$ . At ambient room temperature, the API remains suspended in the middle of the liquid medium.

### Microscopic Evaluation of MDI Product

Microscopic evaluation (SEM using a Hitachi S-3500N, Hitachi high technologies, Gaithersburg, MD, 5-kV accelerating voltage, magnification of 1000 $\times$ ) of representative MDI samples was performed to qualitatively evaluate the particle size and shape of the MDI spray before and after temperature cycling.

### Cascade Impaction Testing of MDI Product

The aerodynamic PSD of the MDI was obtained using the Mark II Andersen Cascade Impactor (1 AFCM Non-Viable Ambient Particle Sizing Sampler, 28 L/min flow rate, Graseby-Andersen, Smyrna, GA).<sup>[28–30]</sup> A 1-L glass entry port was employed in place of the United States Pharmacopeia (USP) entry port because studies in this laboratory have shown it to provide more sensitivity to changes in the aerodynamic PSD of the suspended API.<sup>[10]</sup> Each MDI test can was fitted with a standard actuator for oral delivery and tested as per a validated cascade impaction method. The sample was shaken and primed prior to testing. Each sample was actuated two times into the impactor, and three samples for each batch/condition were tested.

The API was recovered from the cascade impactor stages and accessories in an appropriate high-performance liquid chromatography (HPLC)-grade solvent, and the API concentration determined via HPLC with spectrophotometric detection. The mass of API on each

stage or accessory was divided by the total amount collected to give the percent of dose for each stage of the apparatus. The mass median aerodynamic diameter (MMAD) and geometric standard deviation (GSD) were estimated based on the USP method.<sup>[30]</sup> The percent of fine particles (%FP) was calculated as the percent of the dose that was  $\leq 4.7 \mu\text{m}$  (impactor stages 3 through filter).

## RESULTS AND DISCUSSION

### Impact of API Particle Size on the Aerodynamic PSD of the MDI Suspension

As shown by the laser diffraction results (Table 1), the particle size of the API employed in the study

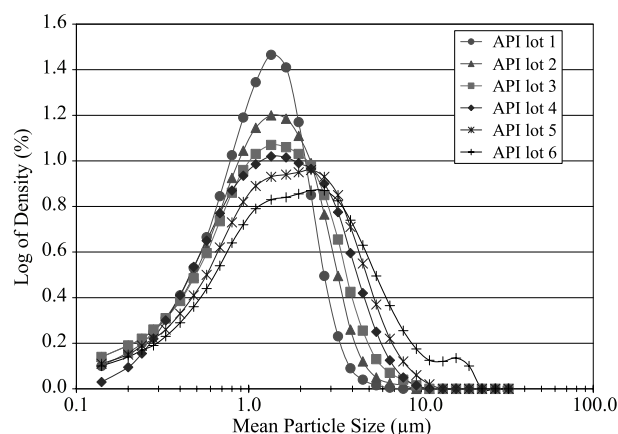


**Figure 1.** Sympatec volume size distribution profiles for API lots.

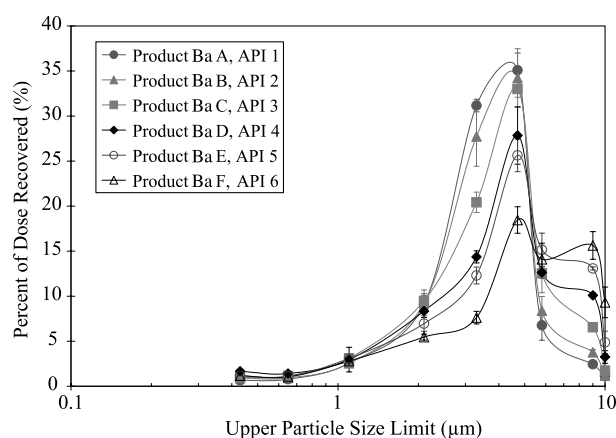


**Figure 2.** Impact of API lot on the aerodynamic PSD of the MDI product.

ranged in median size from 1.14  $\mu\text{m}$  to 1.77  $\mu\text{m}$ . As the median size increased, the volume size distribution by laser diffraction became broader (Fig. 1). The 1.77- $\mu\text{m}$  API lot showed signs of bimodality that may be due to the presence of poorly micronized powder in the sample. The API lots showed little difference in the percent of submicron particles (i.e., 13.2% to 18.1% was  $<0.52 \mu\text{m}$ ; Table 1) and could be better distinguished by the cumulative percent of particles  $<3.00 \mu\text{m}$  (Table 1).

A direct relationship was observed between the MDI-emitted aerosol aerodynamic PSD by Andersen cascade impaction and that of the raw API particle size (Fig. 2;

mean distribution  $\pm$  standard deviation). The MDI product manufactured with API lot 1 (median 1.14  $\mu\text{m}$ ) had a substantially smaller aerodynamic particle size than material manufactured using API lot 6 (median 1.77  $\mu\text{m}$ ). This was particularly manifested in the strong dependence of the %FP and MMAD on the API particle size, such that an increase in the API particle size (i.e., from batch A to batch F) led to a reduction in the %FP and correspondingly larger values for the MMAD (Table 2). A linear relationship was obtained for the %FP ( $\leq 4.7 \mu\text{m}$ ) plotted as a function of the cumulative percent of API particles  $<3.00 \mu\text{m}$  ( $r^2=0.989$ ; Fig. 3; mean distribution  $\pm$  standard deviation). The percent of dose recovered was relatively unaffected by the particle size of the raw API based on the fact that the API collected in the emitted spray was similar for all MDIs tested (Table 2). MDIs made with coarser API had larger amounts of API recovered from the entry port.

The fact that the API impacts the aerodynamic behavior of the product was consistent with the theory predicting that with sufficient evaporation of the propellant, the droplet size can become sensitive to the API component.<sup>[8]</sup> In reported studies where small-size droplets are produced or with the use of a larger-size entry port that allows for more complete droplet evaporation, the aerodynamic PSD has been shown to be sensitive to the API particle size.<sup>[9,10]</sup>

Although the aerodynamic PSD was found to be dependent on API size using cascade impaction, the clinical relevance of the API size in the 1.14  $\mu\text{m}$  to 1.77  $\mu\text{m}$  range needs to be evaluated.

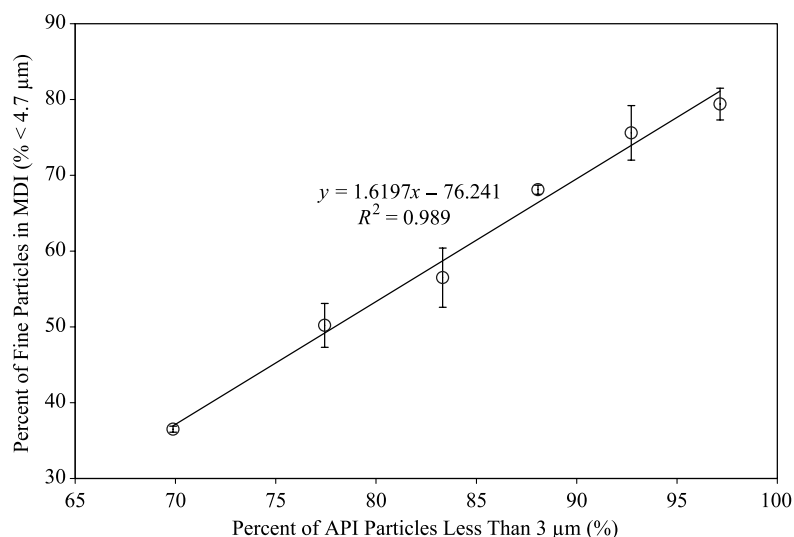


**Figure 3.** Percent of fine particles in MDI as a function of API particle size ( $\% < 3 \mu\text{m}$ ).

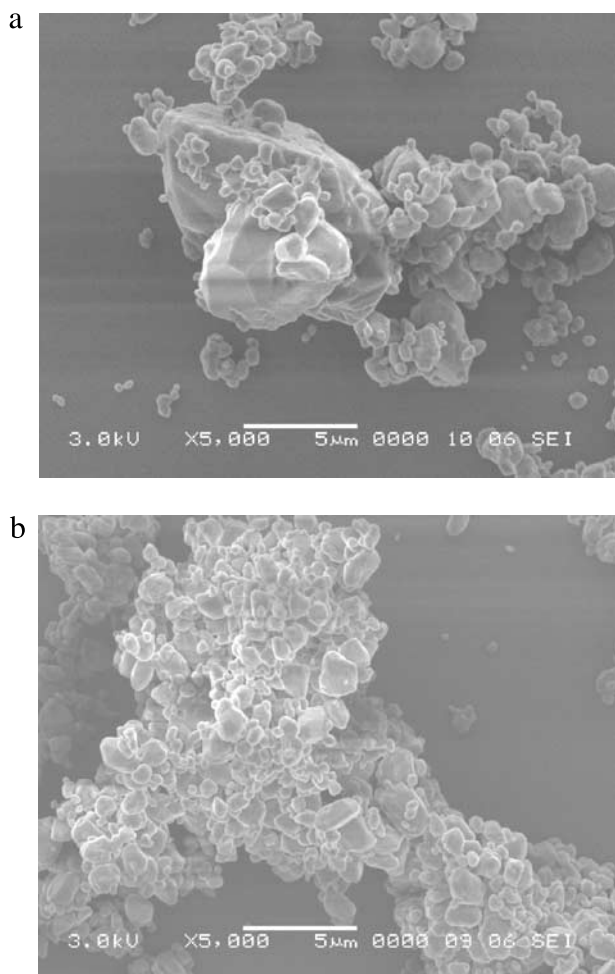


**Figure 4.** Representative SEM images of API at 5,000 $\times$  magnification. (a) Coarse API used in batch G, and (b) fine API used in batch H.

#### Impact of API Particle Size on the Stability of the Aerodynamic PSD of the MDI Suspension After Temperature Cycling

In this part of the study, the stability of MDI aerosol products manufactured with coarse and fine API lots was determined after 2 weeks of temperature cycling (batches G and H, respectively). The fine and coarse API lots had median particle sizes of about 1.1  $\mu\text{m}$  and 1.3  $\mu\text{m}$ , respectively. This size range was selected because it was believed to be representative of that which could potentially be used in an MDI product.

Differences in the size of the API lots were most clearly illustrated in the representative SEM images of the API (Fig. 4), which revealed the presence of larger-size particles in the coarse API lot (used in batch G) compared with the fine API lot (used in batch H).

Before temperature cycling, the percent of dose recovered in the cascade impactor for Batches G and H was similar and therefore relatively independent of the raw API particle size used to manufacture the MDI batch (Table 3). Likewise, the amounts recovered on the stages, entry ports, and casings were similar between the two batches before temperature cycling. Consistent with the previous section, the percent of fine particles and MMAD parameters were quite sensitive to API particle size (Table 3) at the initial time point. The %FP values for the coarse API batch G were 26% lower than that of the fine API batch H. Correspondingly, the MMAD was 38% greater for batch G compared with batch H.

Upon temperature cycling of batch H (made with fine API), an 18% reduction in %FP and 17% increase in MMAD was observed, signaling a shift to larger particle size (Table 3). The overall dose recovery as well as the stage, entry port, and casing recoveries were largely unaffected by the temperature cycling process (Table 3). A more dramatic shift to a larger aerodynamic particle size was observed for batch G (coarse API) as a result of temperature cycling compared with that seen for the batch H (Table 3). For batch G, the %FP was reduced by 52% and the MMAD increased by 57%. For batch G, the shift toward larger aerodynamic particle size with temperature cycling was also manifested by a decrease in the stage recovery and corresponding increase in the entry port recovery (Table 3). Figure 5 (mean distribution  $\pm$  standard deviation) illustrates the larger aerodynamic PSD change that occurs with MDI samples made with coarse API (batch G) compared with that manufactured with fine API (batch H) due to temperature cycling.

The microscopic evaluation (qualitative) of batches G and H suggested that the proportion of larger-size

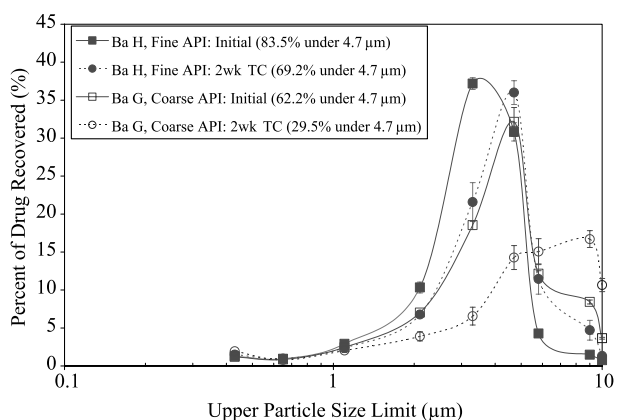


**Figure 5.** Change in cascade impactor PSD profiles for coarse and fine API product batches upon temperature cycling.

particles had increased upon temperature cycling, and that this increase was exacerbated for the coarse API batch (G) compared with the fine API batch (H).

It is suggested that temperature cycling ( $-10^{\circ}\text{C}$  to  $40^{\circ}\text{C}$ ) promotes particle growth for this model formulation as a result of the change in density of the HFA liquid medium with temperature. Thus, the API floats at low temperature and sinks at higher temperature (see "Materials and Methods" section). Therefore, during temperature cycling the API was continually transported (stirring effect) through the liquid medium. This process would be analogous to mixing the API in the medium, a means of aiding particle growth by accelerating the deposition of dissolved molecules on the existing nuclei through the mechanical movement of the solid in the liquid.<sup>[11,13,14,16–18]</sup>

Generally, particle growth that is accelerated by temperature cycling has been attributed to changes in the solubility of the suspended solid as a function of temperature.<sup>[31,32]</sup> The shift to larger particle size is believed to occur as a result of the preferential dissolution of the smaller particles at high temperatures followed by the deposition of the supersaturated solution on the existing particles as the temperature is lowered.<sup>[31]</sup>

In this model formulation, the temperature dependence of the API solubility in the formulation may have contributed to particle growth. A preliminary evaluation of this parameter has shown an inverse correlation of the solubility with temperature, which is contrary to what is normally observed. These results suggest that API solubility could be related to the position of the suspended API in the liquid medium. If the suspended API is floating on top of the liquid, as it is at low temperatures (e.g.,  $<20^{\circ}\text{C}$ ), it may be less prone to nucleation and have greater stability of the supersaturated state. However, if the suspended API is immersed in the liquid medium, as is the case at higher temperatures (e.g.,  $>20^{\circ}\text{C}$ ), nucleation of the dissolved API on the suspended API could more readily occur leading to a reduction in the API solubility.

### Possible Factors Contributing to the Aerodynamic Particle Size Change

#### Proposed Mechanism

Based on the results in the previous section, the increase in aerodynamic PSD upon temperature cycling can be attributed at least in part to the particle size of the suspended API. Size-dependent particle growth, in which larger particles grow more readily than smaller particles, has been observed for a

number of sparingly soluble salts suspended in a liquid medium of low viscosity, particularly when the system was agitated.<sup>[12–14,33–36]</sup> For seed crystals in the size range of about  $0.5\text{ }\mu\text{m}$  to  $100\text{ }\mu\text{m}$ , a linear increase in particle growth with the size of the seed crystal has been observed.<sup>[13,34]</sup> These conditions exist in the present system because the particles were within the predicted size range and mechanical mixing (sedimentation and creaming) was taking place through temperature cycling.

The dominant mechanism that is proposed to describe the size-dependent particle growth involves diffusion of the molecular growth units (e.g., supersaturated liquid) to the solid surface of the seed particle, followed by rate-limiting integration of these growth units onto the particle.<sup>[14]</sup> According to this model, the propensity for growth would be greater for larger-size particles because their repulsion barrier would be smaller,<sup>[14]</sup> whereas the proportion of nucleation sites would be greater on large particles compared with small particles.<sup>[13]</sup> Supersaturation is considered a driving force for this mechanism because it could affect the diffusion of the growth units to the solid surface.<sup>[13,14,17]</sup> As is typical of HFA MDI formulations,<sup>[15]</sup> a cosolvent is employed to dissolve the surfactant, which in this case results in API solubility of  $>0.5\%$  w/w. This level of solubility in the present system may be sufficient to provide the driving force for rate-limiting surface integration.

#### Alternative Mechanism

An alternate mechanism of particle growth involves rate-limiting diffusion of the solid to its nucleation site. This mechanism is proposed when particle growth is inversely related to the particle size and is observed when the majority of particles are submicron in size in a highly supersaturated medium.<sup>[12–14]</sup> When the diffusion of the solid is rate limiting, the process is more energetically favorable for smaller particles.<sup>[12]</sup> At the same time, the energy barrier toward surface integration would be reduced due to the presence of a high density of growth units near the solid surface.<sup>[13,14]</sup> Rate-limiting diffusion was not likely to be favored in this system based on the fact that the suspension particle size did not increase with decreasing size of the API particles. Furthermore, the batches used in this study do not contain a high proportion of submicron particles.

#### Contribution of API Surface Properties

It has been found that particle growth is enhanced by higher length/width axial ratios.<sup>[37]</sup> Moreover,

growth tends to occur at the edge of a particle rather than on the flat surface,<sup>[16]</sup> attributed to the lower surface energy in those positions.<sup>[18]</sup> This could mean that particles with a rougher surface are likely to grow faster than those with a smoother surface.

The coarser API, which was produced by micronizing at a faster feed rate, was shown not only to have a broader PSD than the finer material (Fig. 4), but also likely to have a higher axial ratio and rougher surfaces due to reduced residence time in the micronizer. Typically micronization produces particles that are smoother, rounder, and smaller compared with unm micronized counterparts.<sup>[27]</sup> Thus, a reduction in the micronizer dwell time (i.e., using a higher feed rate) should produce more rodlike and sharper-edged particles.

Although not readily apparent from the microscopic images of the API lots (i.e., Fig. 4), it is still feasible that the coarser API batch could contain generally more rodlike and rougher surfaced material. If this was the case then this factor may have contributed to the increased particle growth in the coarse batch (G) compared with the fine batch (H). Work is underway in this laboratory to characterize the surface properties of micronized API as well as determine their impact on particle growth.

### Polymorphic Transformation

It has been found that particle growth can be enhanced by a polymorphic transformation, particularly when the material has been micronized.<sup>[38–40]</sup> Micronization can lead to crystalline disorder on the surfaces, resulting in the formation of amorphous structures.<sup>[40]</sup> Thus, particles that have undergone micronization may have a higher propensity for particle growth as a result of the greater mobility of molecules at the surface, followed by interparticle bridging.<sup>[40]</sup>

There was no evidence that polymorphic transformation was occurring in this system because the API was found to be purely crystalline (limit of detection of about 1%, see “Materials and Methods” section). Furthermore, the coarse API was less likely to have crystalline disorder on its surfaces and concomitant polymorphic transformation than the fine API because it had less time in the micronizer.

### Primary Nucleation

There was no strong evidence of new nuclei formation in this system. The formation of new nuclei<sup>[18]</sup> tends to occur for relatively dilute systems in which the majority of particles are <500 nm.<sup>[18,41,42]</sup> Because the

majority of particles in this system were in the micron range, it was unlikely that this process occurred.

### Aggregation

It has been found in HFA-based systems that there was an increase in API cohesiveness due to the tendency of the fluorocarbon propellant to self-associate.<sup>[15]</sup> It is speculated that greater particle contact could result in particle growth through fusion of particle surfaces, particularly if the surfaces are metastable. Therefore, this phenomenon could contribute to enhanced particle growth of coarse material by the fact that larger surfaces are generally considered to have stronger interparticle forces, and these materials may also have surface properties that would lead them to be more prone to growth (e.g., contain a higher axial ratio and more rough edges).

Alternatively, the greater cohesiveness of the API could also lead to aggregation, which is not followed by particle growth, but can increase the aerodynamic particle size if the aggregates are not separated during spraying. The latter mechanism has been proposed for a model MDI system containing a high level of insoluble additives in which an increase in the aerodynamic PSD was observed with no evidence of particle growth.<sup>[43]</sup> Thus, size-dependent aggregation cannot be ruled out. Because methods for accurately measuring aggregation in the present MDI system have not yet been developed, it is not possible to determine the contribution of aggregation to the increase in aerodynamic PSD at this time.

## CONCLUSION

This study showed that the particle size of the raw API impacts the properties and stability of the emitted aerosol spray of the MDI. It was found that the aerodynamic PSD of the MDI product was directly related to the particle size of the API used to manufacture the MDI. In addition, under temperature cycling conditions, product manufactured with larger-size API particles had a less stable aerodynamic PSD than that made with smaller-size API particles. Size-dependent particle growth and/or aggregation are believed to be the mechanisms for this increase in aerodynamic particle size during temperature cycling. Because it is critical that the aerodynamic PSD of MDIs be highly reproducible for consistent delivery to the lung, it is important that all factors that affect this parameter be well understood and tightly controlled, including the particle size and physical properties of the API.



## REFERENCES

1. Dolovich, M. Characterization of medical aerosols: physical and clinical requirements for new inhalers. *Aerosol Sci. Tech.* **1995**, 22, 392–399.
2. Elvecrog, J. Metered dose inhalers in a CFC-free future. *Pharm. Tech. Eur.* **1997**, 9 (1), 52–55.
3. Keller, M. Innovations and perspectives of metered dose inhalers in pulmonary drug delivery. *Int. J. Pharm.* **1999**, 186, 81–90.
4. Dolovich, M.B.; Ruffin, R.E.; Roberts, R.; Newhouse, M.T. Optimal delivery of aerosols from metered dose inhalers. *Chest* **1981**, 80 (Suppl.), 911–915.
5. Meyer, K.C.; Auerbach, W. Auerbach, R. Drug delivery to the lung. In *Polymeric Site-Specific Pharmacotherapy*; Domb, A.J., Ed.; John Wiley and Sons: New York, 1994; 347–367.
6. Pritchard, J.N. The influence of lung deposition on clinical response. *J. Aerosol Med.* **2001**, 14 (1), S19–S26.
7. Leach, C.L.; Davidson, P.J.; Boudreau, R.J. Improved airway targeting with the CFC-free HFA-beclomethasone metered-dose inhaler compared with CFC-beclomethasone. *Eur. Respir. J.* **1998**, 12, 1346–1353.
8. Dunbar, C.A. Atomization mechanisms of the pressurized metered dose inhaler. *Part. Sci. Technol.* **1998**, 15 (3–4), 253–271.
9. Berry, J.; Heimbecher, S.; Hart, J.L.; Sequeira, J. Influence of the metering chamber volume and actuator design on the aerodynamic particle size of a suspension metered dose inhaler. *Drug Dev. Ind. Pharm.* **2003**, 29 (8), 865–876.
10. Sequeira, J.; Berry, J.; Sharpe, S.; Naini, V.; Hart, J. A comparison of metered dose inhaler particle size distribution by Andersen cascade impaction using two types of entry ports. *Respir. Drug Deliv. VIII* **2002**, 2, 573–576.
11. Careless, J.E.; Moustafa, M.A.; Rapson, H.D.C. Effect of crystal form, cortisone alcohol and agitation on crystal growth of cortisone acetate in aqueous suspensions. *J. Pharm. Pharmacol.* **1968**, 20 (8), 639–645.
12. Wey, J.S.; Strong, R.W. Influence of the Gibbs–Thomson effect on the growth behavior of AgBr crystals. *Photogr. Sci. Eng.* **1977**, 21 (5), 248–252.
13. Garside, J.; Davey, R.J. Secondary contact nucleation: kinetics, growth and scale-up. *Chem. Eng. Commun.* **1980**, 4, 393–424.
14. Stávek, J.; Ulrich, J. A possible new approach to the better understanding of crystallization kinetics. *Cryst. Res. Technol.* **1994**, 29 (4), 465–484.
15. Tzou, T.Z.; Pachuta, R.R.; Coy, R.B.; Schultz, R.K. Drug form selection in albuterol-containing metered-dose inhaler formulations and its impact on chemical and physical stability. *J. Pharm. Sci.* **1997**, 86 (12), 1352–1357.
16. Noboru, S.; Masaaki, Y.; Akira, S.; Noriaki, K. Growth enhancement and liquid-inclusion formation by contacts on NaCl crystal. *AIChE J.* **1999**, 45 (5), 1153–1156.
17. Kim, K.S.; Kim, J.K.; Kim, W.S. Silica particle growth in metastable supersaturation solution. *J. Mater. Res.* **2001**, 16 (2), 545–552.
18. Mullin, J.W. *Crystallization*, 4th Ed.; Butterworth: London, 2001; pp. 216–288, 181–214.
19. Matthys, H. Chlorofluorocarbon-free aerosol therapy in patients with pulmonary airflow obstruction. *Respiration* **1996**, 63 (3), 321–324.
20. Byron, P.R.; Miller, N.C.; Blondino, F.E.; Visich, J.E.; Ward, G.H. Some aspects of alternative propellant solvency. *Respir. Drug Deliv. IV* **1994**, 239–242.
21. Vervaet, C.; Byron, P.R. Drug-surfactant-propellant interactions in HFA-formulations. *Int. J. Pharm.* **1999**, 186, 13–30.
22. Cummings, R.H. Pressurized metered dose inhalers: chlorofluorocarbon to hydrofluoroalkane transition-valve performance. *J. Allergy Clin. Immunol.* **1999**, S230–S235.
23. McDonald, K.J.; Martin, G.P. Transition to CFC-free metered dose inhalers—into the new millennium. *Int. J. Pharm.* **2000**, 201, 89–107.
24. Hixon, L.M. Select an effective size-reduction system. *Chem. Eng. Prog.* **1991**, 87 (5), 36–44.
25. Miranda, S.; Yaeger, S. Homing in on the best size reduction method. *Chem. Eng.* **1998**, 105 (12), 102–110.
26. Miranda, S. Advances in powder micronization technology for the pharmaceutical industry. *J. Pharm. Proc.* **1997**, 18 Nov Sup.
27. Akbarieh, M.; Tawashi, R. Morphic features of solid particles after micronization in the fluid energy mill. *Int. J. Pharm.* **1987**, 35, 81–89.
28. Milosovich, S. Particle size determination via cascade impaction. *Pharm. Technol.* **1992**, 16, 82–86.
29. Johnsen, M.A. Properties of aerosol particles. *Spray Technol. Mark.* **1992**, 2 (8), 46–55.
30. General chapter 601. United States Pharmacopeia. **2001**, 25, 1969–1980.
31. Careless, J.E. A study into the prediction of mass transfer. *J. Pharm. Pharmacol.* **1976**, 28 (8), 2.
32. Ziller, K.H.; Rupprecht, H. Control of crystal

- growth in drug suspensions. *Pharm. Technol. Drug Stab.* **1989**, 118–131.
33. White, E.T.; Bendig, L.L.; Larson, M.A. The effect of size on the growth rate of potassium sulfate crystals. *AIChE Symp. Ser.* **1976**, 153 (72), 41–47.
  34. Yushan, R.; Qiu, T.; Yuanmou, Z. A study on the growth kinetics of small crystals of KCl. *Process Technol. Proc.* **1984**, 2, 289–292. (Ind. Crystallization).
  35. Jones, A.G.; Budz, J.; Mullin, J.W. Crystallization kinetics of potassium sulfate in an MSMR agitated vessel. *AIChE J.* **1986**, 32 (12), 2002–2009.
  36. Combes, C.; Freche, M.; Rey, C. Nucleation and crystal growth of dicalcium phosphate dihydrate on titanium powder. *J. Mater. Sci., Mater. Med.* **1995**, 6 (12), 699–702.
  37. Phillips, E.M.; Byron, P.R.; Dalby, R.N. Axial ratio measurements for early detection of crystal growth in suspension-type metered dose inhalers. *Pharm. Res.* **1993**, 10 (3), 454–456.
  38. Ravin, L.J.; Shami, E.G.; Rattie, E.S. Physical-chemical evaluation of 3-(3-hydroxy-3-methylbutylamino)-5-methyl-as, Triazino [5,6-b] Indole. *J. Pharm. Sci.* **1970**, 59 (9), 1290–1295.
  39. Halebian, J.K. Characterization of habits and crystalline modification of solids and their pharmaceutical applications. *J. Pharm. Sci.* **1975**, 64 (8), 1269–1288.
  40. Ward, G.H.; Schultz, R.K. Process-induced crystallinity changes in albuterol sulfate and its effect on powder physical stability. *Pharm. Res.* **1995**, 12 (5), 773–779.
  41. Auer, S.; Frenkel, D. Suppression of crystal nucleation in polydisperse colloids due to increase of the surface free energy. *Nature* **2001**, 413 (6857), 711–713.
  42. Verdoes, D.; Kashchiev, D.; van Rosmalen, G.M. Determination of nucleation and growth rates from induction times in seeded and unseeded precipitation of calcium carbonate. *J. Cryst. Growth* **1992**, 118 (N3–4), 401–413.
  43. Berry, J.; Kline, L.C.; Naini, V.; Chaudhry, S.; Hart, J.L.; Sequeira, J. Influence of the valve lubricant on the aerodynamic particle size of a suspension metered dose inhaler. Manuscript submitted for publication.

Copyright of Drug Development & Industrial Pharmacy is the property of Marcel Dekker Inc. and its content may not be copied or emailed to multiple sites or posted to a listserv without the copyright holder's express written permission. However, users may print, download, or email articles for individual use.

Copyright of Drug Development & Industrial Pharmacy is the property of Taylor & Francis Ltd and its content may not be copied or emailed to multiple sites or posted to a listserv without the copyright holder's express written permission. However, users may print, download, or email articles for individual use.